PCCP

Accepted Manuscript

ROYAL SOCIETY OF CHEMISTRY

www.rsc.org/pccp

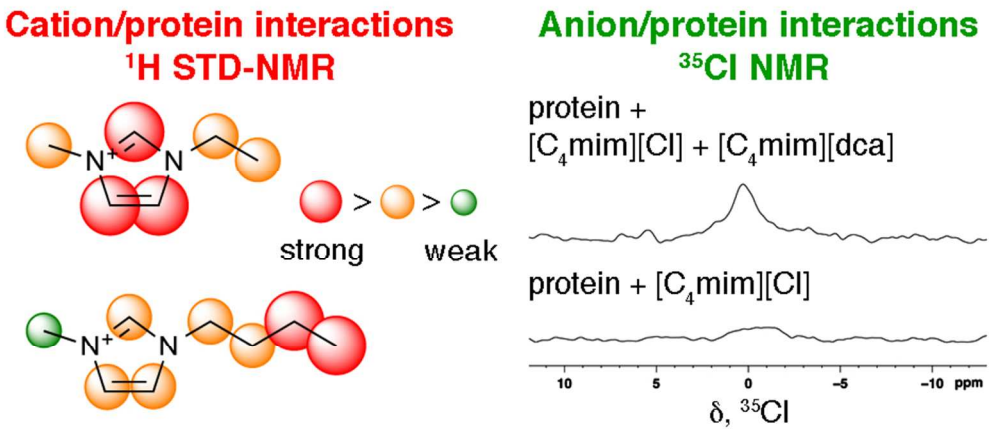

The influence of imidazolium-IL cation and anion on HSA destabilisation was investigated at atomic detail by a combination of STD-NMR and ^{35}Cl NMR.
80x34mm (300 x 300 DPI)

Epitope mapping of imidazolium cation in ionic liquid-protein interactions unveils the balance between hydrophobicity and electrostatics towards protein destabilisation

Micael Silva[a], Angelo Miguel Figueiredo[a*], Eurico J. Cabrita[a*]

[a] REQUIMTE, CQFB, Departamento de Química, Faculdade de Ciências e Tecnologia, Universidade Nova de Lisboa, Quinta da Torre, 2829-516 Monte de Caparica, Portugal

Corresponding Author

am.figueiredo@fct.unl.pt; ejc@fct.unl.pt

Graphical Abstract

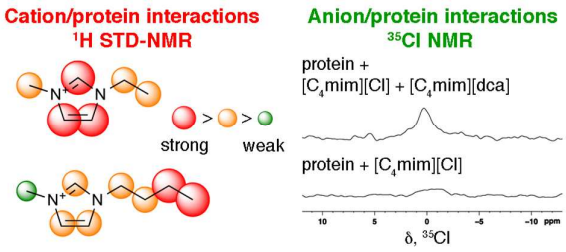

Text for Graphical Abstract

The influence of imidazolium-IL cation and anion on HSA destabilisation was investigated at atomic detail by a combination of STD-NMR and ^{35}Cl NMR.

ABSTRACT

We investigated imidazolium-based ionic liquid (IL) interactions with human serum albumin (HSA) to discern the level of cation interactions towards protein stability. STD-NMR spectroscopy was used to observe the imidazolium ILs protons involved in direct binding and to identify the interactions responsible for changes in T_m as accessed by differential scanning calorimetry (DSC). Cations influence protein stability less than anions but still significantly. It was found that longer alkyl side chains of imidazolium-based ILs (more hydrophobic) are associated with a higher destabilisation effect on HSA than short-alkyl groups (less hydrophobic). The reason for such destabilisation lies on the increase surface contact area of the cation with the protein, particularly on the hydrophobic contacts promoted by the terminus of the alkyl chain. The relevance of the hydrophobic contacts is clearly demonstrated by the introduction of a polar moiety in the alkyl chain: a methoxy or alcohol group. Such structural modification reduces the degree of hydrophobic contacts with HSA explaining the lesser extent of protein destabilisation when compared to longer alkyl side chain groups: above $[C_2mim]^+$. Competition STD-NMR experiments using $[C_2mim]^+$, $[C_4mim]^+$ and $[C_2OHmim]^+$ also validate the importance of the hydrophobic interactions. The combined effect of cation and anion interactions was explored using ^{35}Cl NMR. Such experiments show that the nature of the cation has no influence in the anion-protein contacts, still the nature of the anion modulates the cation-protein interaction. Herein we propose that more destabilising anions are likely to be a result of a partial contribution from the cation as a direct consequence of the different levels of interaction (cation-anion pair and cation-protein).

INTRODUCTION

In recent years, Protein-Ionic Liquid (P-IL) interactions have been the subject of intensive studies mainly because of IL ability to be used as solvents for biochemical reactions [1] and their capability to promote folding/unfolding of proteins [2–7] avoiding formation of molecular aggregates [5]. However, most of the reported data concerns the effect of ILs on the native structure of proteins in the form of denaturation or stabilisation and little attention has been given to the molecular details of how ILs interact with the biomolecules. From the large spectrum of ILs, concomitant with its tailoring nature, the combination of cations and anions make this issue a daunting question [8]. This raises the intriguing question of whether each ion (cation or anion) is responsible for the stabilising/destabilising phenomena, and whether or how the balance between charge (electronegativity) and hydrophobicity contribute to protein destabilisation.

It is known that high concentrations of some ILs in solution can induce protein unfolding [5,9–12], much like urea [13] and GndHCl [14] despite other ILs can be used without perturbing significantly the protein structure or even have a stabilising effect. Several examples of the effects of various ILs on protein stability have been reported in the literature for ribonuclease A [7] and serum albumins, whether human or bovine [15,16]. The impact of the combination of different pairs of cations and anions of a range of imidazolium or bromide-based ILs on the thermal stability of proteins have been reported by differential scanning calorimetry [7]. Generally, the variations of anionic moiety of ILs have a more obvious effect on protein properties than the cation variations do. Apart the results indicating that the ions of ILs have specific roles in disrupting protein structure and driving aggregation, the effect of cation charge/hydrophobicity and length has never been ruled out.

In our previous studies we have addressed the nature of P-IL interactions focusing on protein structural modifications and specific P-IL interactions [17]. We have shown that protein destabilisation is a consequence of a direct effect of the IL interaction with the polypeptide chain governed by a combination of hydrophobic and electrostatic interactions dictated by the charge at the protein surface. The IL cation and anion have different effects on structure and stability; denaturing interactions with the anion are dominant and dictate the overall stability but the anion effect can be partially overcompensated by combination with a suitable cation. Thus, cation effects cannot be disregarded as suggested also by other studies using imidazolium-based ILs [7].

Wang and Chen [16] have reported the effect of imidazolium based ILs with different alkyl lengths showing that short chain ILs, incapable of aggregation are prone to unfold bovine serum albumin (BSA) in the studied concentration regime. According to the authors, thermodynamic stability between ILs and BSA show that the interaction is entropically driven by predominantly hydrophobic and electrostatic interactions of imidazolium, leading to the unfolding of BSA [16]. Apart from this relation between the loss of secondary and tertiary structure of BSA and hydrophobic and electrostatic interaction, the authors did not present an atomistic mechanism showing which parts within the imidazolium cation (head or tail) are responsible for the contacts that ultimately led to protein unfolding. Interestingly, for those imidazolium-based ILs with longer alkyl chains, protein exposure to concentrations above 1 M generally result in significant unfolding without subjecting the protein to elevated temperatures, however according to Heller [15] such specific behaviour can be attributed to the cation-anion pair. To expand the level of understanding of P-IL interactions, particularly in terms of the nature of specific contacts established with IL cations we have studied the interaction of a set of imidazolium ILs with human serum

albumin (HSA). HSA is the most abundant globular protein in the circulatory system and has been one of the most extensively studied proteins with ILs [10]. The structural aspects of unfolding have been studied by EPR [10], fluorescence measurement [16] and SANS [15] showing that HSA irreversibly aggregates and unfolds in imidazolium based ILs, revealing subtle differences in the interaction of the ILs and guanidine hydrochloride (a powerful denaturant) with the protein.

In this work we assessed the influence of cation chain length, compactness and hydrophobicity on the stability of HSA relating it with the degree and nature of P-IL interactions. Using a set of imidazolium-ILs with different alkyl substituents and functionality, the level and nature of P-ILs interactions responsible for the observed stabilisation/destabilisation events on HSA were explored using an integrated biophysical approach. Combining saturation transfer difference (STD) NMR results with calorimetric data (melting temperatures, T_m) from differential scanning calorimetry (DSC) we characterise the type of IL interactions that most contribute towards protein stability. STD-NMR spectroscopy is a highly versatile technique for NMR-based ligand studies that allow to identify a binding compound in a mixture, as well as to define the protons of the ligand which contribute more for the interaction with the protein, known as epitope mapping [18,19].

Using imidazolium-cation based ILs with two different anions known to have a moderately destabilising effect (Cl^-) and a strong denaturing effect (dicyanamide – dca^-) (Scheme 1) we investigate the role of the anion on the cation-protein interaction. The modulation of anion-protein interaction by the different cations was indirectly monitored by ^{35}Cl NMR linewidth, which is sensitive to exchange between bulk-free and protein-bound Cl^-. Different responses in ^{35}Cl linewidths allow us to discern how anion-protein interactions are affected by the nature of the cation. Overall, we show

that the thermal stability of HSA in the different IL solutions combined with NMR spectroscopy makes possible to understand and discern the nature of interactions established between cation and/or anion in the denaturing process of HSA. Understanding such interactions will not only provide information on the denaturation and renaturing capacity of ILs on proteins contributing significantly to a better understanding of the role that salts in general play in many biotechnological processes.

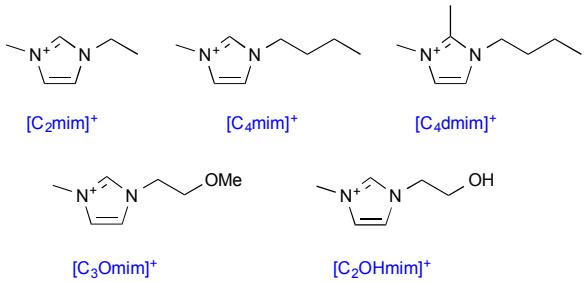

Scheme 1 – Structures of the imidazolium-based ionic liquids cations used in this work.

EXPERIMENTAL

Materials

Lyophilised human serum albumin (HSA) was purchased from Fluka with a purity of 99% and was dialysed to remove any excess or presence of salts. 1-ethyl-3-methylimidazolium chloride [C_2mim][Cl], 1-ethyl-3-methylimidazolium dicyanamide [C_2mim][dca], 1-butyl-3-methylimidazolium chloride [C_4mim][Cl], 1-butyl-3-methylimidazolium dicyanamide [C_4mim][dca] were purchased from IoliTec (Denzlingen, Germany); and, 1-(2-hydroxyethyl)-3-methylimidazolium chloride [C_2OHmim][Cl], 1-(2-hydroxyethyl)-3-methylimidazolium dicyanamide [C_2OHmim][dca], 1-butyl-2,3-dimethylimidazolium chloride [C_4dmim][Cl] and 1-(2-methoxyethyl)-3-methylimidazolium chloride [C_3Omim][Cl] (product I, 025-01) were purchased from Solchemar. All ILs were at least 99% pure, and were dried for 24 h under vacuum at 60 °C. pH values are direct meter readings uncorrected for any isotope effects.

NMR Spectroscopy

NMR experiments were acquired at 298K in a Bruker Avance II+ spectrometer operating at a proton Larmor frequency of 600 MHz with a 5 mm TCI cryoprobe. Sample protein concentration was 50 μM in 99.9% D_2O up to a total volume of 500 μl; ionic liquid concentration was 5 mM, pH meter reading pH 7 (uncorrected for deuterium isotope effect). Saturation transfer difference (STD) experiments were prepared with a molar excess of ionic liquid of 100, i.e. protein:IL ratio of 1:100. Such ratios are typical to obtain reasonable amplification factors for weak binding ligands [19,20]. The STD-NMR spectra were acquired with 64K data points in t_2 and 512 scans in a spectral window of 12335.53 Hz centred at 2824.03 Hz. An excitation-

sculpting module with gradients was employed to suppress the water proton signals. Selective saturation of the protein resonances (on resonance spectrum) was performed by irradiating at −1 ppm using a series of Eburp2.1000-shaped 90° pulses (50 ms, 1 ms delay between pulses) for a total saturation time of 1.5 s. For the reference spectrum (off resonance), the samples were irradiated at 20000 Hz. Proper control experiments were performed with the reference sample (absence of protein) in order to optimize the frequency for protein saturation (−1 ppm) and to ensure that the IL ligand signals were not affected. NMR data was processed and analysed in Bruker's Topspin^{TM} 3.2 and intensities from 1D STD-NMR spectrum was obtained by subtracting the on resonance spectrum from the off resonance. In all cases, to accomplish the epitope mapping of each ionic liquid ligand, the STD-NMR intensities were normalized with respect to that with the highest response, i.e. the relative STD-NMR with the highest intensity was set to 100 % as a reference, and all other STD-NMR signals were calculated accordingly. STD-NMR spectra were analysed by the amplification factor (A_{STD}), calculated by multiplying the relative STD-NMR effect (($I_0 - I_{SAT}$)/I_0) with the molar ratio of ligand in excess relative to the protein (protein:IL ratio = 100), where I_0 and I_{SAT} are the intensity of the signals in the reference and saturated spectra, respectively. Consequently, ($I_0 - I_{SAT}$) is the peak intensity in the STD-NMR spectrum (I_{STD}). For the competition studies we used the $[C_2mim]^+$ *vs*. $[C_2OHmim]^+$ and $[C_2mim]^+$ *vs*. $[C_4mim]^+$. The ratio of protein/IL was kept to 1:100 for each IL and the solutions were prepared as above.

^{35}Cl NMR

The ^{35}Cl NMR measurements were performed at 298 K on a Bruker Avance II+ 400 spectrometer operating at 39.204 MHz using a 5mm broadband tuneable probe.

Spectra were collected with standard 1D using a 90° pulse for chloride with the following acquisition parameters: spectral width of 2354 Hz, digitized into 1K data points with a 90° pulse length of about 13.5 μs. A delay of at least 10 T_1 was used for all of the measurements. The NMR probe temperatures were checked using ethylene glycol or methanol. For the ^{35}Cl titration experiments small amounts of a stock solution of protein-ionic liquid (50 μM HSA + 5 mM IL) were added to a freshly prepared 50 μM HSA sample in 99.9% D_2O. The volumes added were 10, 20, 30, 50, 75, 100, 150, 225, 300 and 360 μl of stock solution to the freshly prepared HSA without IL. This guarantee that the concentrations of the studied chloride-ILs were kept constant through the NMR experiment as well as the amount of water, but the amount of protein concentration was gradually increased. In the competition between [C_4mim][Cl] and [C_4mim][dca] to a 50 μM sample of HSA it was added 5 mM of each IL, respectively.

NMR Diffusion Experiments

The self-diffusion of HDO was used as an internal reference to account for viscosity effects upon protein addition in the ^{35}Cl NMR studies. Diffusion measurements were performed using the stimulated echo sequence using bipolar sine gradient pulses and eddy current delay before the detection [21]. Typically, in each experiment 32 spectra of 64K data points were collected, with a duration of the magnetic field pulsed gradients (δ) of 3 ms, a diffusion time (Δ) of 100 ms, and an eddy current delay set to 5 ms. The gradient recovery time was 200 μs. The sine shaped pulsed gradient (g) was incremented from 5 to 95 % of the maximum gradient strength in a linear ramp. Data were analysed using the variable gradient fitting routines in Bruker's Topspin™ 3.2 software and in all cases HDO resonances were fit to a single exponential decay

function using peak intensities. For standard deviation purposes three different diffusion experiments were done for each sample.

Differential Scanning Calorimetry

To examine thermodynamically the degree of IL perturbations in HSA we performed differential scanning calorimetry (DSC) using a Microcal VP-DSC (General Electric, Fairfield, CT). With that we are able to measure the excess heat capacity of HSA unfolding as a function of temperature and directly calculate the calorimetric enthalpy of thermal unfolding in the different ionic liquids under study (Scheme 1) and though the corresponding melting temperatures associated. Samples for DSC analysis were prepared exactly with the same concentrations as described above for the STD-NMR experiments and were degassed prior to any DSC measurement to avoid bubble formation during the temperature scan. A scan rate of 90 °C/h, from 25 to 95 °C with an equilibration period of 20 min was used, with a constant cell pressure of approximately 2 atm. Buffer baseline scans were established prior to analysis of each HSA – IL under study by performing 20 consecutive heating and cooling scans in both the sample and reference cells until the scans deviated less than 0.0003 kcal/°C. Before each measurement the cells were exhaustive cleaning. Samples were scanned through two consecutive heating and cooling cycles. Data were analysed with the Origin version 6.0 software package with the Microcal VP-DSC. Sample scans were buffer-subtracted, concentration normalised, corrected with the progress baseline option, and fitted by nonlinear least squares analysis using a two-state model option with two independent transitions. The resulting fitted excess heat capacity curves yielded the melting temperatures (T_m) for each IL under study and are reported in

Table 1. Errors were determined from the standard deviation fitted curve of the two scans.

RESULTS AND DISCUSSION

HSA Stability in imidazolium-based ILs

The literature has systematically characterised the effect of imidazolium-based ILs as strong denaturants [7,17] through the thermal stability of proteins (T_m). Since we known a priori that anion effect on protein stability is largely dominant [2,7,22] cations still were observed to play a significant role on protein stability. The already described destabilising cation effect behaviour from $[C_2mim]^+$ < $[C_4mim]^+$ < $[C_6mim]^+$ with consequently decrease in the melting temperature (T_m) might be explained by the structural features of the cation, particularly hydrophobicity and charge. The positive charge concentrated at the imidazolium ring might exert a stabilising effect, whereas long alkyl chains more prone to hydrophobic interactions might be associated with a destabilization effect. The balance between these could influence the nature of interactions established within ILs and the protein. Yet it is difficult to relate the observed effects to specific features of the cation. In order to study the effect of ion size, surface charge density and hydrophobicity the series of cations depicted in Scheme 1 were investigated. These imidazolium cations vary in their size and hydrophobicity according to the nature of the alkyl substituents in position 3 of the imidazolium ring.

A detailed understanding regarding the stability of HSA in the presence of these cations was performed by differential scanning calorimetry (DSC) using the moderate destabiliser Cl^- derived ILs and the same IL:protein ratios as used in the following NMR studies. The thermodynamic data obtained can be linked to the capacity of cations in perturbing the melting temperatures and the enthalpy of HSA. The thermal

assays in different imidazolium-based ILs aqueous solutions are compared to aqueous solution (Fig. 1). Fig. 1 represents DSC thermogram of HSA in water and in the presence of different ionic liquids under study. The DSC profiles include two thermodynamic transitions where cooperative unfolding is present: one transition for temperature below 55 °C and another for temperatures above 65 °C. According to literature the first pre-denaturation transition is due to reversible conformational changes that occur before unfolding while the second transition corresponds to the thermal unfolding, via an irreversible process [23]. In water it was proposed that the first transition includes three sequential sub-transitions related to HSA domain separation and concomitant structural perturbations [24].

When compared to water in the presence of ILs the changes obtained in the thermogram suggest that the pre-denaturation transitions are more affected than the thermal unfolding. The interaction of ILs with HSA is a complex process that includes electrostatic interactions and hydrophobic effects that contribute to conformational changes and destabilisation. The perturbations in the curve profile for the first transition suggest that the ILs induce strong conformational changes that lead to changes in the number of sub-transitions. On the other side, the effects of the ILs in the thermal unfolding temperature are only marginal at the low working concentrations. At higher concentrations the T_m effects are clearer but despite that the T_m rank for the different ILs is maintained. Since in the presence work ILs were used as probes to understand the nature of interactions responsible for the denaturing process of HSA, the thermal unfolding transition temperature (T_m) is more relevant for the following discussion.

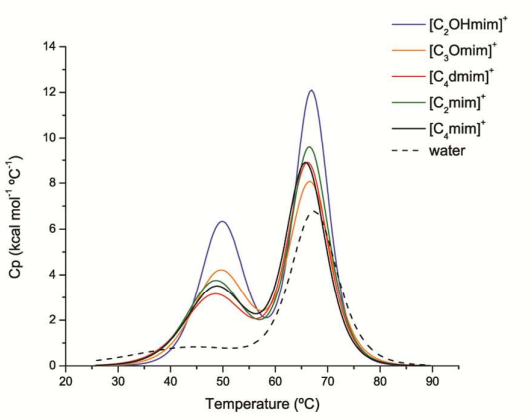

Fig. 1 Baseline subtracted, heat capacity curves for HSA in chloride imidazolium-based ionic liquids and in water observed by differential scanning calorimetry.

Table 1 Transition temperature T_m for the thermal denaturation of HSA determined by DSC for the different imidazolium-based cations under study

	T_m (°C)
[C_4mim][Cl]	65.91 ± 0.06
[C_4dmim][Cl]	66.29 ± 0.06
[C_2mim][Cl]	66.62 ± 0.04
[C_3Omim][Cl]	66.71 ± 0.08
[C_2OHmim][Cl]	66.95 ± 0.05
Water	67.51 ± 0.06

As seen on Table 1 the denaturing transitions tend to progressively shift towards lower temperatures following the order Water > $[C_2OHmim]^+$ > $[C_3Omim]^+$ > $[C_2mim]^+$ > $[C_4dmim]^+$ > $[C_4mim]^+$. Apparently, HSA tends to be destabilised by more hydrophobic cations. Though, $[C_4mim]^+$ causes significant unfolding of the native structure of HSA and is the strongest destabiliser (see Table 1). Interestingly,

the data shows a correlation between cation hydrophobicity and destabilising propensity, the more polar cation having the less destabilising effect. This correlation with cation hydrophobicity is the same as reported previously on Im7 [17] and on RNase [5,7]. Similarly, as mentioned above the same destabilising effect with increased chain length is also observed. The DSC data supports our previous findings concerning the possibility of tuning the destabilising effect of the anion by the cation. The destabilising effect by itself does not allow inferring about the strength and nature of the cation protein interaction. The chosen cations allow to probe different levels of interactions: the less hydrophobic cation $[C_2OHmim]^+$ is prone to be involved in hydrogen bonds through the hydroxyl group, the $[C_3Omim]^+$ has a similar size to $[C_4mim]^+$ however due to the OMe group is more polar. Indeed, $[C_4mim]^+$ is the most hydrophobic cation on the series while $[C_2mim]^+$ is more compact and due to its smaller size should be more susceptible to electrostatic interactions with the negatively charged surface of HSA. Therefore, to further understand the molecular determinants of the cation contribution to protein stability we mapped the interactions sites in the cation structure using STD-NMR spectroscopy.

HSA-IL interactions mapped by STD-NMR Spectroscopy

Using STD-NMR spectroscopy as a tool to detect binding epitopes of imidazolium-based ILs (Scheme 1) with HSA we assess which atoms (hydrogen) of the cation interact more strongly with the protein. The same series of chloride derived ILs as used in the DSC measurements were studied.

Representative STD-NMR spectra of $[C_2mim]^+$ and $[C_4mim]^+$ are shown in Fig. 2 (the complete set of STD-NMR spectra are available as ESI, Fig. S1-S6) and the

overall results for all ILs are graphically mapped into the ILs structure in Fig. 3, except for [C_2OHmim][Cl] (see further discussion).

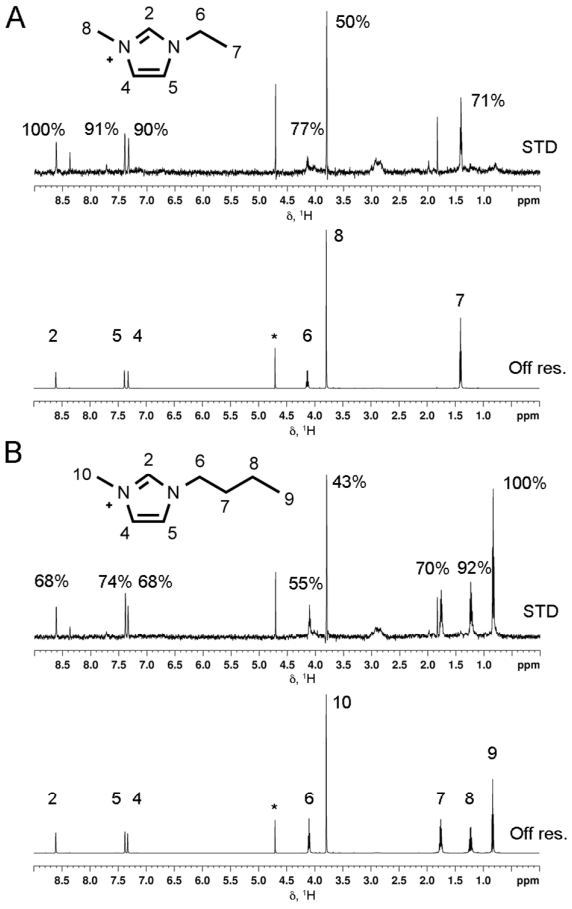

Fig. 2 (A) Top – STD NMR spectrum of 5 mM [C_2mim][Cl] with 50 μM human HSA and relative STD NMR intensities in percentage; Bottom – Reference spectrum (off resonance) with resonance assignments. (B) As in (A) for 5 mM [C_4mim][Cl] with 50 μM human HSA.

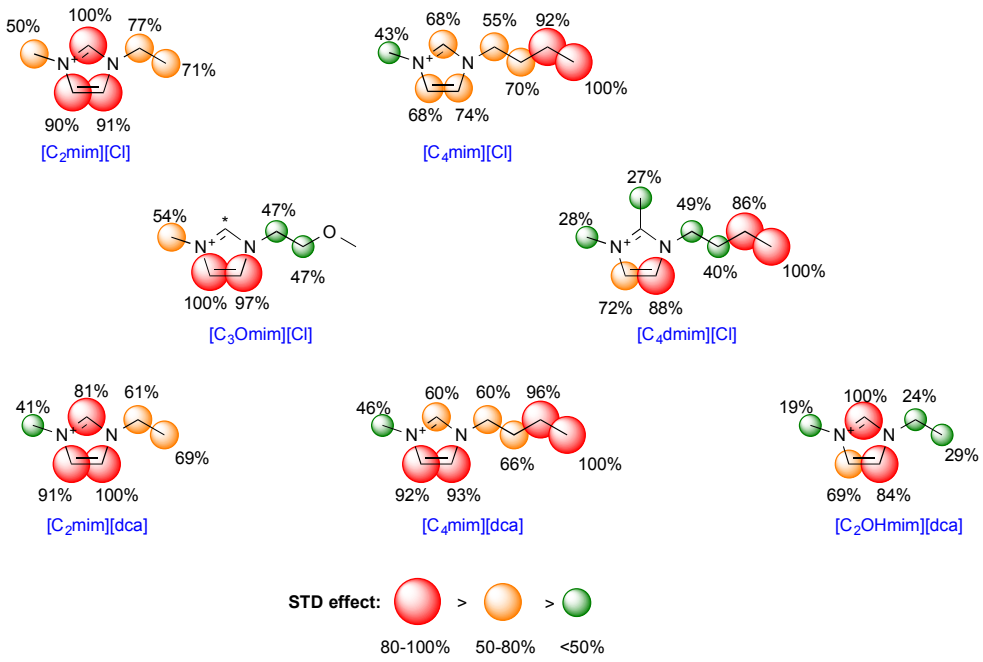

Fig. 3 Epitope mapping obtained for the different ILs under study in the presence of HSA. (* proton exchanges with D_2O)

As can be depicted in Fig. 2 different levels of STD-NMR responses are obtained from the cation moiety of the IL. For both ILs all protons show STD-NMR, a clear indication that the cations establish direct interaction with the protein.

The comparison of the STD-NMR responses with the reference spectrum for each IL, allows the determination of the relative STD-NMR responses and the epitope mapping as represented in Fig. 3. When considering these percentages there is a clear difference in the pattern of interaction between $[C_2mim]^+$ and $[C_4mim]^+$ cations. While in the $[C_2mim]^+$ the interaction is predominantly with the core of the aromatic imidazolium ring (100% STD-NMR for proton 2 and proton 4 and 5 around 90%), in the $[C_4mim]^+$ the pattern of interaction shifts to the extended alkyl chain, with the maximum STD-NMR observed for the terminal methyl group of the butyl chain. Once the HSA isoelectric point is bellow 5, the main driving force for the protein-

cation interaction should be electrostatic in nature, and that would justify the higher STD-NMR response from the imidazolium ring protons. The results obtained for $[C_4mim]^+$ suggests that besides electrostatic, hydrophobic interactions are also important, most probably because they increase the probability of interaction with the protein surface. Therefore an IL cation such as $[C_4mim]^+$ capable of interacting by both mechanisms is more destabiliser as shown by the DSC data. Assuming that the P-IL interactions are non-specific, the shift of the STD-NMR contacts from the ring to the alkyl chain might indicate that the number of possible sites for hydrophobic interaction is greater.

To further validate these ideas we also explore in detail the STD-NMR contact maps with other cations: $[C_4dmim]^+$, $[C_3Omim]^+$ and $[C_2OHmim]^+$. Since $[C_2OHmim]^+$ is the less destabiliser and the less hydrophobic cation, the comparison with $[C_2mim]^+$ and $[C_4mim]^+$ is very useful to validate the idea that increase protein destabilisation by imidazolium cation based IL is mainly associated to hydrophobic contacts. In $[C_2OHmim]^+$ the presence of an OH group at the edge of the alkyl chain alters completely its hydrophobic character. From the STD-NMR spectra (see ESI Fig. S3) we see that the detected contacts are at the protein background level. Since all experiments were done exactly under the same conditions (i.e. protein concentration, IL:protein ratio and STD-NMR parameters were the same in all experiments) this result suggests that the interaction is the weakest of all. Such results are remarkable and fit nicely with previous CD and UV/Vis measurements on lysozyme by Mann and co-workers [6]. Apparently, lysozyme in the presence of cations with ethanol side chain have found a pronounced stability at high temperatures, while the same IL with propyl instead of ethanol led to spontaneous denaturing of the enzyme at 75% wt [6].

In the $[C_3Omim]^+$ cation the OH group was changed into a OMe group and the detected interaction pattern is similar to what was previously observed for the $[C_2mim]^+$ cation, with the highest STD-NMR response in the imidazolium ring.

From $[C_4mim]^+$ to $[C_4dmim]^+$ the introduction of an extra substituent in the imidazolium ring (methyl group) at position 2 does not alter significantly the epitope of the interaction, and the maximum STD-NMR is still observed at the terminus of the alkyl chain (see Fig 3). Nevertheless, the DSC data shows that the T_m obtained for $[C_4dmim]^+$ is higher than for $[C_4mim]^+$. The reason for that could be that despite having similar hydrophobicity there are still differences relative to the possibility of establishing hydrogen bonds. $[C_4mim]^+$ has the possibility of interacting by hydrogen bond through H2 and most probably of being more disruptive of the protein structure.

As we have shown in a previous study some level of specificity for P-IL interactions might exist depending on the nature of the exposed surface residues [17] however in the context of STD-NMR we consider the interactions to be non specific because there are multiple binding sites and the STD-NMR response is the result of the contribution of all interaction sites. Our results show that imidazolium ILs destabilise proteins, as larger are the contacts established in the P-IL system. Increasing the alkyl chain length with concomitant hydrophobicity prompts a destabilisation effect on protein from: $[C_2OHmim]^+ < [C_3Omim]^+ < [C_2mim]^+ < [C_4dmim]^+ < [C_4mim]^+$. Nevertheless, is interesting to note that, not only the cation ring of imidazolium contributes to the P-IL interaction. The elongation of the alkyl chain on $[C_4mim]^+$ delocalise the strongest contacts from the imidazolium ring towards the terminal position of the methyl group. Leading to a variation in the ability of the ILs to destabilise HSA. Indeed, a direct correlation should exist between the level and the nature of interaction with protein stability, and just that could explain the

T_m values obtained (see previous discussion on DSC section). Though, we may read cations in terms of decreasing T_m values from: $[C_2OHmim]^+$ (less interactions, mainly electrostatic) < $[C_3Omim]^+$ < $[C_2mim]^+$ < $[C_4dmim]^+$ < $[C_4mim]^+$ (more interactions, electrostatic and hydrophobic). Such level of interaction is apparently due to a balance between electrostatic attraction along with the hydrophobic interaction, between the alkyl side chain plus imidazolium ring, and the hydrophobic peripheral domain of HSA.

As mentioned before, we known *a priori* that anion effect on protein stability is largely dominant [2,7,22] therefore in order to probe if the anion interferes in the protein-cation interaction, the three main cations $[C_2OHmim]^+$, $[C_2mim]^+$ and $[C_4mim]^+$ combined with the strongly destabilizer dca^- anion were investigated. Remarkably for dca^- anion $[C_4mim]^+$ show a different contact pattern compared to the chloride anion. The delocalisation of the higher intensity STD-NMR contacts from the imidazolium ring to the terminus of the alkyl chain observed in the chloride derivatives when going from $[C_2mim]^+$ to $[C_4mim]^+$ is not observed for dicyanamide and a similar STD intensity is observed for both moieties in [C_4mim][dca] (Fig. 3). Indeed the combination of $[C_4mim]^+$ with the dca^- anion affects the cation contacts with the protein extending the contact surface of the IL with the protein. The same is true for the combination [C_2OHmim][dca] for which contacts are now detected, probably due to the more hydrophobic character of the dca^- anion compared to Cl^-. This reinforces the idea that cation-anion interactions are crucial to the balance of interactions established between ion pairs and ion-solvent that determine protein stability.

For $[C_2mim]^+$ no significant changes in the relative STD-NMR responses as compared with chlorine derivatives were observed (Fig. 3). Overall these results

validate the idea that anion interactions are the main driving force for protein destabilisation and that might even perturb the cation interaction.

A direct evidence of the relative strength of anion interaction was also obtained using [C_2mim][$EtOSO_3$]. The STD-NMR experiment with this IL allows observing simultaneously cation-protein and anion-protein interactions (Fig. 4). Indeed the STD-NMR spectrum is completely dominated by the response from anion protons; comparatively the cation STD-NMR response is so weak that remains in the noise level.

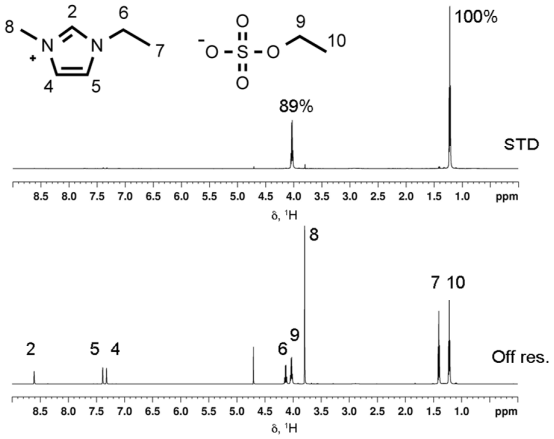

Fig. 4 Top – STD NMR spectrum of 5 mM [C_2mim][$EtOSO_3$] with 50 μM human HSA and relative STD NMR intensities in percentage; Bottom – Reference spectrum (off resonance) with resonance assignments.

Furthermore to probe if the cation interferes in the protein-anion interaction a set of experiments based on the observation of ^{35}Cl linewidths and intensities was performed, as discussed in the next section.

Anion-protein interaction - ^{35}Cl NMR

Once STD-NMR data has shown cations interacting directly with the protein, we find it would be important to understand and validate if such observable interactions could be mediated by anions, using another experimental approach. Using our imidazolium-based ILs cation series (Scheme 1) we study the binding properties of the quadrupolar chloride anion to the protein. ^{35}Cl NMR signal lines are broadened by quadrupolar relaxation associated with binding of the anion to protein once they are in exchange between the free- and the bound-form [25]. Fast chemical exchange of Cl^- between bound and free (hydrated) states averages the different relaxation rates and linewidths. At the extremely narrowing limit a single Lorentzian line is observed, only dependent of the free and bound state populations.

In all aqueous IL solutions studied in the absence of HSA, ^{35}Cl linewidths are relatively narrow (Fig. 5 and Fig. S9-S13). The spectra of HSA containing solutions are several fold-broader but only a signal line is observed. As stated above, such broadening is characteristic of the binding of Cl^- to HSA at the extreme narrowing limit. Successive increases in the HSA concentration decreases the ratio of free:bound chloride, which can be followed by the increase in the ^{35}Cl linewidth and decrease in peak intensity (Fig. 5). The peak broadening is accompanied by a corresponding decrease in the ^{35}Cl signal height because the bound chloride experiences the shorter relaxation time of the protein. Therefore, peak height ratio represents an easily measurable response of chloride binding that can be described in terms of the NMR peak height for free- and bound-states. The dependence of the ^{35}Cl NMR signal upon HSA addition is shown in Fig. 5 for [C_4mim][Cl] and in Fig. S9-S13 (ESI) for the other cations, and are graphically represented as peak heights decays in Fig 5B. To confirm that the line broadening effect is not due to viscosity changes caused by

increased protein concentration, the self-diffusion coefficient of HDO was determined for the solutions containing 0, 21.75 and 50 μM HSA (see ESI Table S1). Since viscosity and diffusion are inversely related according to the Stokes-Einstein equation, any changes in viscosity can be directly monitored using a diffusion probe as HDO [26]. For $[C_4mim][Cl]$ solutions the value determined was 1.67×10^{-9} ($\pm$ 0.01) m^2/s, independent of protein concentration (see ESI Table S1). The fact that the HDO diffusion coefficient remains constant upon protein addition on all ILs means that the variations in solution viscosity are minimal and do not account for the ^{35}Cl line broadening.

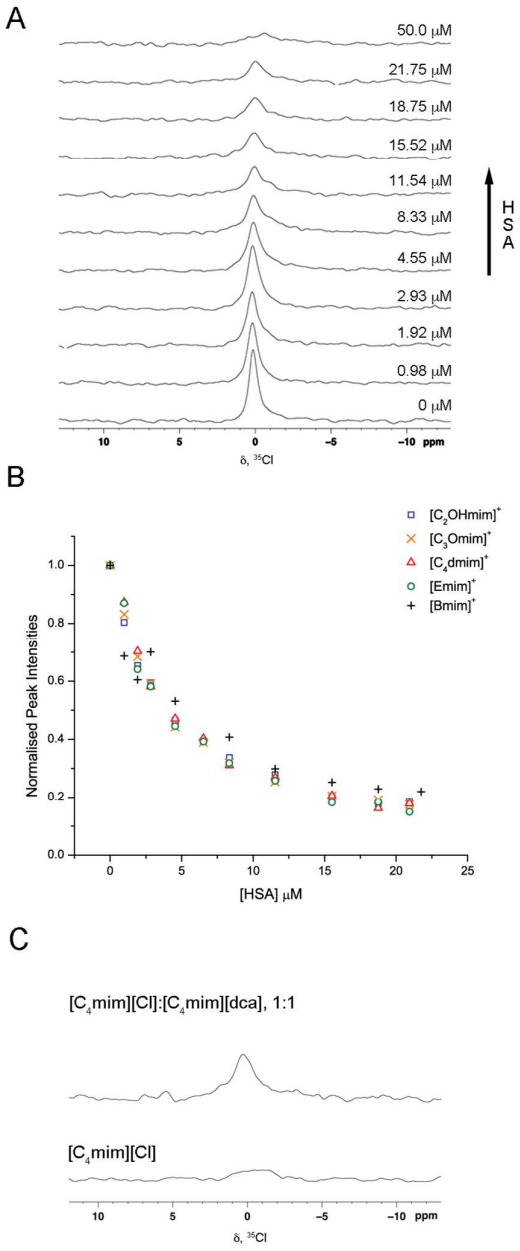

Fig. 5 (A) Effect of HSA addition on the ^{35}Cl resonance of a sample containing 5 mM $[C_4mim][Cl]$ in D_2O (500 μL). Increased HSA concentration was achieved through the addition of small volumes of 50 μM HSA, 5 mM $[C_2mim][Cl]$ to maintain the total concentration of chlorine constant. (B) dependence of the relative ^{35}Cl peak height ratio ($I_{[HSA]}/I_{free}$) upon HSA addition. (C) ^{35}Cl NMR competition experiment between $[C_4mim][Cl]$ and $[C_4mim][dca]$.

The similar behaviour of the peak intensity decay (Fig. 5B) and linewidth broadening (see ESI, Fig. S9-S13) for the different ^{35}Cl NMR titrations reveals no significant differences within the imidazolium-ILs. This suggests that the protein-cation interaction does not interfere with the anion-protein interaction. Therefore, cation and anion effects on protein stability can be accounted separately.

To confirm the strong denaturing capability of dca^- due to direct interaction with the protein we have performed a competition experiment with Cl^-. In a $[C_4mim][Cl]$ solution containing sufficient HSA to broaden completely the ^{35}Cl signal, the same molar amount of $[C_4mim][dca]$ was added (Fig 5C). Remarkably, the ^{35}Cl NMR signal was partially recovered after addition of $[C_4mim][dca]$, meaning that Cl^- binding sites were occupied by stronger interacting dca^- anion with concomitant increase on the free Cl^-. This result shows that direct anion interactions with the protein are in the origin of the destabilising effects observed.

Cation/cation-protein interaction competition

To investigate the relative strength of interaction of different cations the binding epitopes were examined in competition STD-NMR experiments using two ILs at the same time: $[C_2mim]^+$ *vs*. $[C_2OHmim]^+$ and $[C_2mim]^+$ *vs*. $[C_4mim]^+$ - see ESI, Fig. S7-S8. Relative STD intensities were calculated for all protons that receive saturation transfer and the higher response was normalised to 100% allowing a direct comparison of the individual responses from both cations. Overall, for each imidazolium cation the protons that give STD response in the competition experiments are not significantly different from the individual STD NMR experiments (Fig. 3).

For the $[C_2mim]^+$ *vs*. $[C_2OHmim]^+$ the core of ion interactions with the protein is still in the imidazolium ring (Fig. S7, ESI), yet the $[C_2OHmim]^+$ responses are weaker in intensity, confirming that the introduction of an -OH group is responsible for a relative decrease in the level of contacts. In the $[C_2mim]^+$ *vs*. $[C_4mim]^+$ competition there are significant peak overlap that preclude a detailed analysis of the epitope relative to the imidazolium ring. However, the terminal alkyl chain methyl group from $[C_4mim]^+$ is well resolved and shows the maximum STD intensity. All that reinforces the idea that $[C_4mim]^+$ interacts more strongly with HSA (*via* alkyl chain) than $[C_2mim]^+$.

The significance of the alkyl chain length

Shu *et al*. [16] using UV-Vis and fluorescence have shown that short alkyl chains of imidazolium-based ILs were responsible for protein structural perturbations. But it proved difficult to evaluate the degree of interactions established between alkyl side chains with protein and if there is any cause that could contribute towards the destabilisation. Surprisingly, Shu *et al*. [16] using $[C_4mim]^+$ and $[C_4bim]^+$ - i.e. two butyl groups symmetrically distant at each terminus of the cation ring - state that the hydrophobicity of $[C_4bim]^+$ been larger due to the longer length of the alkyl chain, still no differences could be observed on the UV-Vis spectra of BSA when compared to $[C_4mim]^+$ (see Figure 1 from ref. [16]). They suggest that the side chain of imidazolium-based ILs poses no influence on the interactions between ILs and BSA. From our perspective their approach by UV-Vis could not certainly distinguish unambiguously the role of imidazolium alkyl side chains since both molecules pretty resemble the same feature, i.e. a butyl group at one or both terminus of the imidazolium cation ring. Though, the important hydrophobic character provided by

the alkyl chain length could not be addressed correctly once both were butyl. Indeed, in our work the STD-NMR data clearly evidences the level of interactions established within HSA and the imidazolium alkyl side chains, and is in accordance with EPR measurements [10]. As Akdogan *et al*. [10] reported, as the length of the alkyl chain attached to imidazolium-based ILs is increased from $[C_2mim]^+$ to $[C_6mim]^+$ the spectral contribution of freely tumbling fatty acids increased significantly, indicating that the competitive uptake of imidazolium-based ILs into hydrophobic channels of the protein, was preferentially by larger alkyl chains, in other words the hexyl component of imidazolium-based IL was the most effective in releasing fatty acids attached to HSA. From our STD-NMR data it is clear that most of the interactions are definitely from the alkyl side chain, particularly when the alkyl group is longer than ethyl ($-C_2H_5$), see Fig. 3. Longer alkyl groups from imidazolium-based ILs will certainly compete with hydrophobic, non-polar patches of the protein driving to its inherent destabilisation. Simultaneously, the presence of –OH and $–O–CH_3$ groups reduce the level of alkyl side chain interactions between the imidazolium ILs and HSA underpin the importance of the cation ring to the interaction on this type of ILs.

CONCLUSIONS

Up to now, the interactions between proteins and ILs in aqueous media are not well understood and the underlying interpretations are still mostly speculative. HSA at pH above its isoelectric point (4.7 at 25 °C) is fully soluble where in interaction with ILs can experience topological and conformational changes [11]. The reasons of those changes are in the core of how ionic liquids interact with biomolecules contributing therefore for its stability. Despite many studies have stated protein stability in IL media in terms of solubility, polarity and viscosity effects, few have characterised protein surface charge intimately linked with IL hydrophobicity and electrostatic. In this context surface charge on proteins is intimately linked with preferential exclusion and direct binding mechanism of ILs ions [16,17,27]. The amphiphilic distinctive nature of imidazolium-ILs is what makes them so special on protein stability studies. When concerning the cation, they contain a charge polar moiety and a hydrophobic moiety, typically an alkyl chain. The polar head group of the imidazolium cation helps solubilise the IL despite the presence of the alkyl chain. Is this complex net of ions that might disrupt hydrogen bonding, non-polar interactions and electrostatic interactions that will certainly affect protein stability. Therefore, is not surprising that the change in cation hydrophobicity by varying the length of the alkyl group and the introduction of other functional groups will have immediate consequence in the nature of ion-pair, and fundamentally in the ability to interact with the protein. The elongation of the alkyl side chain length in imidazolium-based ILs leads to an augment in the ILs hydrophobicity and hence an increase in the P-IL interaction complexity. With increasing IL complexity (mainly, chain length and hydrophobicity) imidazolium ILs may restrict protein conformational changes as we observed previously on Im7 protein [17]. This

conformational restriction caused by ion interaction creates some stiffness in the three-dimensional structure and though a more compact structure. Thus an increase in the alkyl chain length of cations leads to destabilisation of native protein hydrophobic interactions alongside with a greater degree of binding. However, ILs with hydroxylated cations as choline, or imidazolium-based cations with functionalised –OH side chains or –OMe side chain, with less degree of protein interactions are more biocompatible simply because they hold the water mimicking property and hydrogen bonding functionality, helping protein conformational dynamics; an idea supported by previous studies [4,6,28]. In other words, such ILs allow more 'freely' available water molecules surrounding the protein surface stimulating the hydrogen-bond strength of interfacial water having a similar behaviour as bioprotective osmolytes [29]. On the other hand, increasing the number of attractive hydrophobic interactions between the protein and the imidazolium-IL the unfolded state is thermodynamically favoured compared to the native state due to its larger solvent accessible surface area. Therefore the diversity of cation/anion combinations in ILs allows a great versatility of properties that alter protein stability as macromolecular crowders, bioprotective osmolytes or chemical denaturants.

Overall, in HSA the driving force for imidazolium cation-polypeptide interaction should involve electrostatic interactions between the negatively charge protein surface at working conditions (pH ≈ 7) and the imidazolium cation. Such interactions depend on the nature of the anion, since disrupting the ion-pairing interaction is necessary to establish protein stabilising/destabilising interactions. Thus, according to hydrophobicity cations can interact weakly and non-specifically with HSA. Indeed, only the most weakly hydrated anions accumulate around protein. This can be understood in light of the different binding sites for cations and anions within

HSA – imidazolium cations with larger and longer hydrophobic alkyl chains are more protein destabilisers. As noted by Akgogan [10] and shown experimentally in this work, the side chain length is the key binding site for imidazolium cations to (de)stabilise proteins. When the positive charge is localised in a smaller imidazolium cation ($[C_2mim]^+$) the nature of P-IL contacts are preferably through the cation ring, less destabilising HSA within the same anion type. On the other hand, increasing the chain length by methylene groups, will not only alleviate the ring charge, distributing more the charge density, as well as increase cation hydrophobicity throughout the ion – more destabiliser effect. The result will be for such longer alkyl side chain imidazolium-based ILs to establish preferentially interactions with HSA hydrophobic moieties, resulting in a serious distortion in the protein conformation [10,16].

Overall, the structures and energetic of P-IL interactions will depend on a whole host of factors that induce changes in the protein free energy. The protein sequence (including hydrophobicity, charge and propensity for different types of secondary structure) will determine the nature of the binding sites for ILs in conjunction with the type of IL (imidazolium-like or ammonium-like, length of alkyl chain and the ratio between protein and IL).

ACKNOWLEDGEMENTS

We gratefully acknowledge the Fundação para a Ciência e a Tecnologia (project RECI/BBB-BQB/0230/2012 and CQFB Strategic Project PEst-C/EQB/LA0006/2013) for their financial support. The NMR spectrometers are part of The National NMR Facility, supported by Fundação para a Ciência e a Tecnologia. We thank Prof. Helena Santos group (ITQB-UNL) for providing access to DSC equipment.

NOTES AND REFERENCES

Electronic Supplementary Information (ESI) available: full spectra of STD-NMR experiments for [C_4dmim][Cl], [C_3Omim][Cl], [C_2OHmim][Cl], [C_4mim][dca], [C_2mim][dca], [C_2OHmim][dca] and competition STD-NMR experiments for [C_2mim][Cl] *vs*. [C_4mim][Cl] and [C_2mim][Cl] *vs*. [C_2OHmim][Cl]. ^{35}Cl NMR spectra for [C_2mim][Cl], [C_4mim][Cl], [C_4dmim][Cl], [C_2mim][Cl], [C_4dmim][Cl], [C_3Omim][Cl] and [C_2OHmim][Cl] titrations with HSA. NMR diffusion experiments to guarantee that increased protein concentration over ^{35}Cl titration did not change ILs solution viscosities.

1. J.-Q. Lai, Z. Li, Y.-H. Lü, and Z. Yang, *Green Chem*, 2011, **13**, 1860–68.
2. K. Fujita, D. R. MacFarlane, and M. Forsyth, *Chem Commun*, 2005, 4804–6.
3. N. Byrne, L.-M. Wang, J.-P. Belieres, and C. A. Angell, *Chem Commun*, 2007, 2714–6.
4. K. Fujita, D. R. MacFarlane, M. Forsyth, M. Yoshizawa-Fujita, K. Murata, N. Nakamura, and H. Ohno, *Biomacromolecules*, 2007, **8**, 2080–6.
5. D. Constatinescu, C. Herrmann, and H. Weingärtner, *Phys. Chem. Chem. Phys.*, 2010, **12**, 1756–63.
6. J. P. Mann, A. McCluskey, and R. Atkin, *Green Chem*, 2009, **11**, 785–92.

7. D. Constantinescu, H. Weingärtner, and C. Herrmann, *Angew Chem Int Ed Engl*, 2007, **46**, 8887–9.

8. M. Klähn, G. S. Lim, A. Seduraman, and P. Wu, *Phys. Chem. Chem. Phys.*, 2011, **13**, 1649–62.

9. G. A. Baker and W. T. Heller, *Chem Eng J*, 2009, **147**, 6–12.

10. Y. Akdogan, M. J. N. Junk, and D. Hinderberger, *Biomacromolecules*, 2011, **12**, 1072–9.

11. T. Singh, P. Bharmoria, M. Morikawa, N. Kimizuka, and A. Kumar, *J Phys Chem B*, 2012, **116**, 11924–35.

12. X. Wang, J. Liu, L. Sun, L. Yu, J. Jiao, and R. Wang, *J Phys Chem B*, 2012, **116**, 12479–88.

13. A. Das, R. Chitra, R. R. Choudhury, and M. Ramanadham, *Pramana*, 2004, **63**, 363–368.

14. S. N. Baker, H. Zhao, S. Pandey, W. T. Heller, F. V Bright, and G. A. Baker, *Phys. Chem. Chem. Phys.*, 2011, **13**, 3642–4.

15. W. T. Heller, *J Phys Chem B*, 2013, **117**, 2378–83.

16. Y. Shu, M. Liu, S. Chen, X. Chen, and J. Wang, *J Phys Chem B*, 2011, **115**, 12306–14.

17. A. M. Figueiredo, J. Sardinha, G. R. Moore, and E. J. Cabrita, *Phys. Chem. Chem. Phys.*, 2013, **15**, 19632–43.

18. C. A. Lepre, J. M. Moore, and J. W. Peng, *Chem Rev*, 2004, **104**, 3641–76.

19. B. Meyer and T. Peters, *Angew Chem Int Ed Engl*, 2003, **42**, 864–90.

20. A. Viegas, J. Manso, F. L. Nobrega, and E. J. Cabrita, *J Chem Educ*, 2011, **88**, 990–994.

21. D. H. Wu, A. D. Chen, and C. S. Johnson, *J Magn Reson A*, 1995, **115**, 260–4.

22. H. Weingärtner, C. Cabrele, and C. Herrmann, *Phys. Chem. Chem. Phys.*, 2012, **14**, 415–26.

23. G. A. Picó, *Int J Biol Macromol*, 1997, **20**, 63–73.

24. M. Rezaei Tavirani, S. H. Moghaddamnia, B. Ranjbar, M. Amani, and S. A. Marashi, *J Biochem Mol Biol*, 2006, **39**, 530–6.

25. N.-H. Ge, W. S. Price, L.-Z. Hong, and L.-P. Hwang, *J Magn Reson*, 1992, **97**, 656–660.

26. E. J. Cabrita and S. Berger, *Magn Reson Chem*, 2001, **39**, S142–8.

27. E. M. Nordwald and J. L. Kaar, *J Phys Chem B*, 2013, **117**, 8977–86.

28. C. Lange, G. Patil, and R. Rudolph, *Protein Sci*, 2005, **14**, 2693–701.

29. S. N. Timasheff, *Annu Rev Biophys Biomol Struct*, 1993, **22**, 67–97.